Neutron-scattering study of the "one-dimensional" conductor $K_2Pt(CN)_4Br_{0.3}\cdot 3.2D_2O$ (KCP)

J. W. Lynn, M. Iizumi,* and G. Shirane
Brookhaven National Laboratory,† Upton, New York 11973

S. A. Werner and R. B. Saillant
Scientific Research Staff, Ford Motor Company,‡ Dearborn, Michigan 48121

(Received 26 March 1975)

The triple-axis neutron technique has been used to make a detailed temperature-dependent study of the scattering associated with the $2k_F$ instability discovered by Comes *et al.* and subsequently studied by Renker *et al.* in the "one-dimensional" (1-D) conductor $K_2Pt(CN)_4Br_{0.3}\cdot 3.2D_2O$ (KCP). At low temperatures, they found that the elastic scattering on the planes perpendicular to the conducting c axis at $Q_z = 2k_F$ was confined to relatively narrow peaks, and that with increasing temperature these peaks became diffuse perpendicular to $\vec{c}$. We find that the elastic scattering can be quantitatively described by assuming there are static (or quasistatic) charge-density waves (CDW) in the parallel $Pt(CN)_4$ chains, with a temperature-dependent interchain correlation length. The observed asymmetry of the scattering perpendicular to $\vec{c}$ is due to the variation of the structure factor of the $Pt(CN)_4$ complexes, which respond as a unit to the CDW. At elevated temperatures, the elastic scattering approaches the 1-D form expected for uncorrelated CDW's in "chains" of $Pt(CN)_4$. The temperature variation of the amplitude of the CDW in each chain is obtained from the data, and is found to decrease slowly with increasing temperature above 80 K. The width of the scattering along the chain direction remains very narrow at all temperatures, and for $T \lesssim 160$ K a lower limit to the intrachain correlation length of 300 Å has been set. The inelastic scattering in the vicinity of the $2k_F$ instability extends to lower energies than previously observed and in fact appears to fall to $E \approx 0$ for all temperatures in the range 80–300 K. We interpret these results to indicate that at room temperature the CDW distortion has already manifested itself in the lattice, and that the development of interchain correlations at low temperatures is not directly related to a Peierls-type transition.

I. INTRODUCTION

Mixed-valence planar compounds (MVPC) of the transition metals and the charge-transfer salts of tetracyanoquinodimethane (TCNQ) have recently generated considerable interest because of their one-dimensional (1 – D) electrical properties.[1] These materials share the basic characteristic that their compositions lead to the formation of parallel and widely separated "chains" which can be fairly good conductors of electricity. The MVPC such as KCP [$K_2Pt(CN)_4Br_{0.3}\cdot nH_2O$], for example, have tetragonal lattices which are composed of planar sheets of $Pt(CN)_4$ complexes. This stacking results in a Pt-Pt distance (2.87 Å) along the c axis which is only slightly larger than the nearest-neighbor distance in pure Pt metal, while the interchain distance is 9.87 Å. Based on having 0.30 Br per formula unit, simple band-theory arguments predict that these chains of Pt atoms will form a band from the d_{z^2} orbitals which is 0.85 full, and hence 1 – D metallic properties might be expected.

Electrical-conductivity measurements at room temperature confirmed this 1 – D metallic behavior. The ratio of the conductivity parallel and perpendicular to the c axis is of the order of 10^5, and the magnitude of the conductivity is consistent with the 1 – D band theory. This simple picture was further substantiated by optical measurements which showed metalliclike reflectivity for light polarized parallel to the c axis and a dielectric response for light polarized perpendicular to the c axis. Below room temperature the dc conductivity decreases rapidly and at low temperatures these types of materials are all good insulators. The optical measurements on KCP, however, show qualitatively little change[1,2] between 300 and 4.2 K. (The peaks in the optical conductivity broaden with increasing temperature but do not change position.)

For the MVPC the 1 – D electronic properties are now thought to be strongly influenced by the Peierls[3] instability mechanism. Peierls showed that a 1 – D noninteracting electron gas is unstable to a sinusoidal lattice distortion, the distortion lowering the energy of the electrons by splitting the conduction band into empty and filled bands. In the case of KCP, the wave vector of this distortion is expected to be $1.70\times 2\pi/c$ ($c = 5.74$ Å) and planes of scattering consistent with this type of distortion were observed at room temperature by Comes *et al.*[4] via x-ray diffuse scattering. This diffuse scattering was interpreted as either a static Peierls distortion or a (dynamic) giant Kohn anomaly in the phonon spectrum, the latter being expected as a precursor to a Peierls transition.

Renker *et al.*[5] observed a large anomaly in the longitudinal phonon spectrum along the c axis at wave vectors corresponding to $2k_F$ (plus or minus a reciprocal-lattice vector), which they interpreted as a 1 – D Kohn anomaly. The $2k_F$ instability there-

fore appeared to be dynamical in nature at room temperature. One might then expect that at lower temperatures this instability would lead to a phonon condensation and a concomitant metal-semiconductor transition. Comes *et al.*[6] and Renker *et al.*[7] have studied the temperature dependence of the elastic scattering and found that below ~220 K 3 – D correlations begin to develop, and at $T \approx 100$ K a superlattice structure is found. The three-dimensional ordering, however, is incomplete in the sense that full long-range order is not achieved. There has been speculation that this 3 – D ordering is related to a Peierls-type transition.

The x-ray and neutron-scattering results demonstrated that a CDW instability is indeed important in the MVPC systems, but the relationships between the expected phonon condensation at low temperatures, the observed (incomplete) 3 – D ordering and the electrical and optical conductivities have not been established. Moreover, at room temperature an unexpected elastic component of the scattering at $Q_z = 2k_F$ was found, and the connection between the phonon anomaly and this elastic scattering was not clear.

To clarify these points we have carried out elastic and inelastic neutron-scattering measurements as a function of temperature. To gain a perspective of the nature of the scattering, a diagram of the $(1\bar{1}0)$ reciprocal-lattice plane, which is appropriate for the orientation of our samples, is given in Fig. 1. The basic crystal structure is simple tetragonal,[8] and the reciprocal-lattice points are denoted by the solid circles. The elastic-scattering associated with the 1 – D instability is confined to planes which are oriented perpendicular to the chain axis

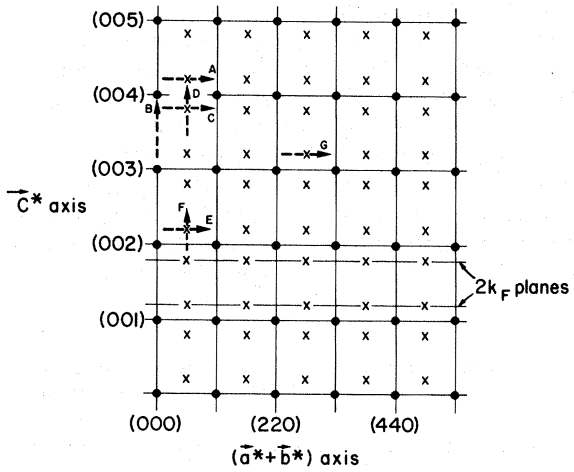

FIG. 1. $(1\bar{1}0)$ scattering plane in the reciprocal lattice of KCP. The solid circles denote the tetragonal reciprocal-lattice points, two of the $2k_F$ planes are shown, and the X's locate the CDW satellite peaks found at low temperatures.

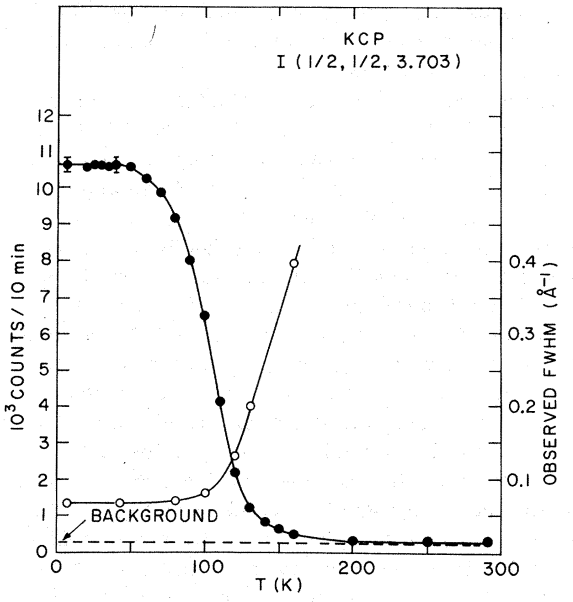

FIG. 2. Peak intensity (solid circles) of the CDW satellite scattering and width (open circles) perpendicular to the c axis as a function of temperature. Long-range correlations develop at low temperatures, but the width of the scattering is still considerably wider than the instrumental resolution. The instrumental resolution is given by configuration A in Table I.

$(\vec{c})$, and a few of these "$2k_F$ planes" are shown. At low temperatures, peaks in the scattering due to 3 – D correlations develop at the intersections of the $2k_F$ planes with the zone boundaries in the [110] direction, and these peaks are denoted by the ×'s. The labeled arrows correspond to positions and directions of various scans we have performed and will be referred to later.

In the course of our investigation we have confirmed many of the general features of the scattering observed by Renker *et al.*[5,7] For example, Fig. 2 shows the character of the CDW satellite scattering as a function of temperature at a scattering vector $\vec{Q} = (0.5, 0.5, 3.703)$. There is a rapid increase of intensity below 120 K which is accompanied by a rapid increase in the interchain correlation length, in agreement with previous measurements. The correlations become fairly long ranged at low temperatures, but the width of the peak perpendicular to $\vec{c}$ is still larger than the instrumental resolution. These data are reminiscent of a phase transition, and although complete long-range order is not achieved we will still refer to this as the "3 – D transition," with $T_{3D} \sim 100$ K. We have found that these data can be quantitatively understood by assuming that there are correlations between the CDW's in the $Pt(CN)_4$ chains, rather than as a Peierls transition. The correlation length along the chains is longer than could be measured at any

temperature,[6] and for temperatures below 160 K we have set a lower limit of 300 Å, which is over 100 Pt – Pt separations.

At room temperature the inelastic scattering shows the 1 – D nature of the $2k_F$ instability found by Renker *et al.*,[5] but the scattering extends to lower energies than previously observed and appears to fall to $E \approx 0$. Thus, the inelastic scattering is connected in a continuous fashion to the elastic scattering along the $2k_F$ planes. As the temperature is decreased the intensity of the inelastic scattering decreases smoothly through T_{3D} with no qualitative change in the phonon spectrum.

Our overview of these results is that at room temperature the physics associated with the CDW state and the 1 – D conducting properties of KCP has already manifested itself in this system. The elastic scattering we observe at room temperature can be described by assuming that there is a CDW distortion in each chain and that these distortions are for all practical purposes uncorrelated with each other. With decreasing temperature in the region of $T \approx 100$ K interchain correlations develop rapidly, but we have not been able to identify a "soft-phonon" mode and in fact no phase transformation takes place. These interchain correlations do not appear to be directly related to the distortion in the chains, as evidenced by the fact that the intrachain correlation length is long enough at all temperatures that it has so far resisted measurement by any technique. The temperature dependences of the electrical and optical conductivities also show no indication of the development of these correlations around 100 K.

II. EXPERIMENTAL PROCEDURES

Both the elastic- and inelastic-scattering measurements were taken on triple-axis neutron spectrometers installed at the high-flux beam reactor at Brookhaven. The monochromator was a "bent" pyrolytic-graphite crystal with the (002) planes oriented for reflection, and the analyzer was a "flat" pyrolytic graphite (002). An energy-analyzing crystal afforded a considerably better signal-to-noise ratio for the elastic-scattering measurements.

A. Resolution

The resolution requirements were quite different for the elastic and inelastic measurements because of the relative intensities of the scattering cross sections. Generally, for the inelastic measurements 40′ full width at half maximum (FWHM) Soller slits were placed before and after the monochromator and analyzer (here denoted by 40-40-40-40) to limit the horizontal divergences of the neutron beams. The incident neutron energy was set greater than the scattered neutron energy. Either the incident or scattered neutron energy was fixed at 14.80 or 13.70 meV so that a pyrolytic graphite filter could be used to remove unwanted higher-order contaminations.

The resolution used for the elastic-scattering measurements will be discussed in more detail, since to compare the data with a model (see Sec. III) the resolution of the spectrometer must be properly taken into account. This is particularly important with regard to extracting the amplitude of the CDW distortion as a function of temperature. The amplitude is related to the intensity of the scattering and this in turn depends on the relative widths in $\vec{Q}$ space of the scattering cross section compared with the resolution. Therefore, care was taken to measure the resolution in order that the convolution of the resolution function with the cross section could be done reliably.

The resolution function is approximately a Gaussian probability distribution[9] in reciprocal space. This distribution depends on the momentum transfer $\vec{Q}$ and incident energy of the neutrons as well as the collimation and the mosaic spreads of the crystals. A few of the instrumental resolution conditions appropriate for our measurements are given in Table I. The FWHM $\vec{Q}$ resolution in two of the $2k_F$ planes is given by δQ_x, δQ_y, δQ_z, where x, y, z are along [110], [1$\bar{1}$0], and [001], respectively. The energy resolution is usually not an important consideration for Bragg scattering, but in this case the "Bragg" scattering at higher temperatures is spread over a plane and is not much stronger than the inelastic scattering. The FWHM energy resolution ΔE is also given in the table. The most comprehensive set of data was taken with the configura-

TABLE I. The FWHM resolution in $\vec{Q}$ and energy at two of the CDW satellite positions. In contrast to the usual convention of Cooper and Nathans [Ref. 9], here x, y, and z are along the crystallographic [110], [1$\bar{1}$0], (vertical resolution) and [001] directions, respectively.

				δQ_x		δQ_y		δQ_z		
Configuration	$\vec{Q}$	E_i (meV)	Collimation	(Å^{-1})	($\sqrt{2}\,2\pi/a$)	(Å^{-1})	($\sqrt{2}\,2\pi/a$)	(Å^{-1})	($2\pi/c$)	δE (meV)
A	(0.5, 0.5, 3.703)	13.70	20-20-20-20	0.031	0.034	0.11	0.12	0.029	0.026	0.40
B	(0.5, 0.5, 3.703)	13.70	40-40-40-40	0.053	0.058	0.11	0.12	0.036	0.033	0.80
C	(0.5, 0.5, 2.297)	4.979	20-20-20-20	0.013	0.014	0.07	0.077	0.008	0.007	0.076
D	(0.5, 0.5, 2.297)	4.979	40-40-40-40	0.021	0.023	0.07	0.077	0.012	0.011	0.152

tion denoted by A. For the measurements with 5.0-meV incident energies a cold (78-K) beryllium filter was placed in the incident beam to filter out higher-energy neutrons.

B. Samples

Two samples were used for the measurements. Both were grown[10] at the Scientific Research Laboratories, Ford Motor Co., and were fully deuterated to eliminate the large incoherent scattering of protons. Each crystal had a volume of ~0.20 cm^3, which is rather small for inelastic-scattering experiments. The mosaic distributions were measured with a "perfect" Ge crystal and were found to be approximately Gaussian in shape with FWHM of 0.63° and 0.42°. They were mounted in an air-tight aluminum container in a heavy-water atmosphere to prevent dehydration. The aluminum container was subsequently mounted in a cold-gas flow cryostat in which temperature stabilization and control of ~0.1 K are routinely achieved. The lattice parameters at liquid-helium temperature were measured to be $a = 9.84$ Å, $c = 5.70$ Å; and at room temperature $a = 9.90$ Å, $c = 5.77$ Å.

The samples were of good quality, but we should point out that we observed some additional weak elastic scattering at positions not expected for the tetragonal lattice or the $2k_F$-CDW distortion. This scattering could not be attributed to higher-order contamination or scattering processes such as multiple Bragg reflections. The strongest peak occurred along the c axis at $\vec{Q} = (0, 0, 3.35)$, and was ~2% of the (002) Bragg peak in one of the crystals. The intensities of these peaks appeared to depend on the thermal history of the samples, and increased with time. This may indicate an additional chemical ordering is occurring. It could also be due to loss of water from the surface, although steps were taken to prevent this. The basic characterizations of the elastic and inelastic $2k_F$ scattering were systematically monitored to determine any changes with time, and no changes were observed. "Extra" scattering has also been reported in x-ray studies.[11]

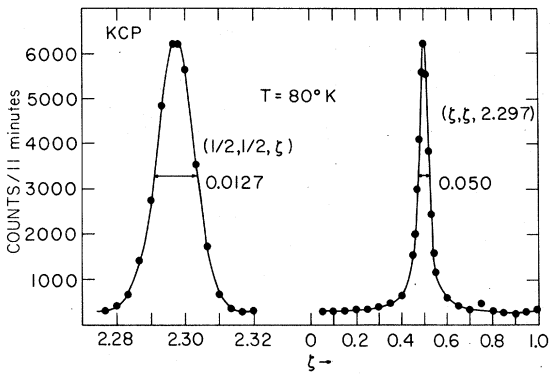

FIG. 3. Observed scattering at the CDW satellite position (0.5, 0.5, 2.297). The scan on the left-hand side is "through" the $2k_F$ plane, i.e., along the c-axis direction. The width is limited by the instrumental resolution, and the position shows that the CDW is incommensurate with the tetragonal lattice. The scan on the right-hand side measures the interchain correlations. $\zeta = 0.5$ is the zone boundary of the tetragonal lattice in the [110] direction. Note the difference in abscissa scale of the two plots of this figure.

III. ELASTIC-SCATTERING RESULTS

The elastic-scattering associated with the CDW's manifests itself as Bragg "planes" which are oriented perpendicular to the chain axis in reciprocal space. That these are planes rather than points is a direct consequence of the 1 – D nature of the sinusoidal distortion. These "satellite" planes intersect the c axis at values of Q_z equal to $2\pi l/c \pm 2k_F$, where l is an integer.

If the CDW's in the chains are not correlated with respect to each other, then the elastic scattering will be spread out on the $2k_F$ planes with a distribution of intensity characteristic of the 1 – D structure factor of a chain of $Pt(CN)_4$ complexes. As the correlations between the chains develop, the scattering will reflect these correlations by forming peaks on the $2k_F$ planes which sharpen as the temperature is lowered. The waves in adjacent chains tend to become 180° out of phase with each other at low temperatures.

The scattering observed in the vicinity of the satellite position $\vec{Q} = (0.5, 0.5, 2.297)$ at 80 K is shown in Fig. 3. These data were taken with an incident neutron energy of 5.0 meV, which gives relatively good instrumental resolution (configuration D of Table I). The scan through the $2k_F$ plane (F of Fig. 1) gives a width which is limited by the instrumental resolution, as does an identical scan with configuration C of Table I. From these measurements we can estimate an upper limit to the intrinsic width of the $2k_F$ planes of 0.006 $Å^{-1}$ FWHM, which corresponds to a correlation length along the chain axis of $\gtrsim 300$ Å, or over 100 Pt atoms. Identical measurements at 120 K show no broadening along the c-axis direction. These results extend the limit of 20 Pt atoms set by Renker *et al.*

The position of the peak locates the $2k_F$ plane, and we find that $2k_F = (1.703 \pm 0.002)2\pi/c$. The CDW is incommensurate with the tetragonal lattice, and measurements from 6.5 to 160 K show no commensurate-incommensurate transition in this temperature range. Above 160 K the measurements become increasingly more difficult, but there is still no indication of a change in the position of the $2k_F$ planes.

Barmatz *et al.*[12] and Menth and Rice[13] have suggested on the basis of acoustic-attenuation and

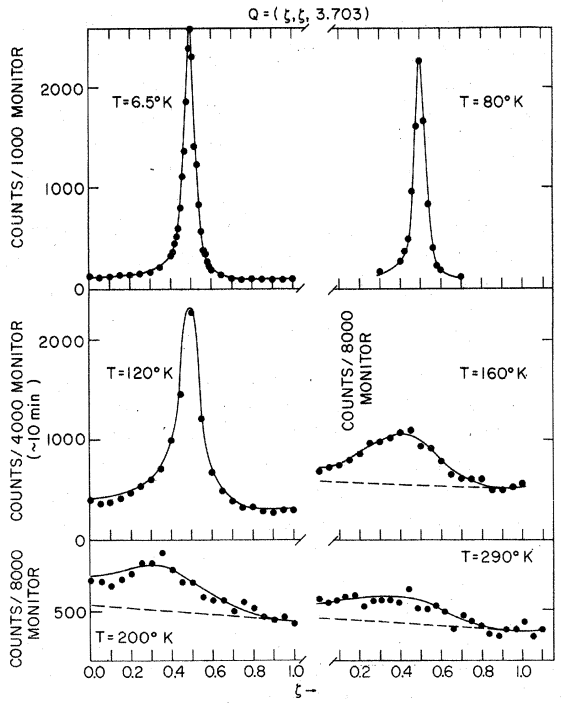

FIG. 4. Temperature dependence of the satellite scattering perpendicular to $\vec{c}$ at a series of temperatures. The solid curves are the fits of the data to the model as explained in the text. Note the pronounced asymmetry and shifts of the peak with increasing temperature. The dashed lines indicate the background (measured separately).

magnetic-susceptibility measurements that there is a phase transformation in KCP for $T \approx 35$–40 K. We have monitored the intensities of the (114) and (004) Bragg peaks in the temperature range 20–50 K and observed no changes. We have also carefully measured the intensity and position of the $2k_F$ satellite peak at $\vec{Q} = (0.5, 0.5, 3.703)$ and found no appreciable temperature dependence in this temperature range. If there is a phase transition near 35 K it does not seem to be related to the $2k_F$-CDW instability.

Figure 3 also shows a scan (E of Fig. 1) along the $2k_F$ plane in the [110] direction. The scattering peaks up sharply at (0.5, 0.5, 2.297), indicating well-developed interchain correlations, although the observed width of the peak is still considerably larger than the instrumental resolution. This peak is approximately Lorentzian, that is, the cross section is of the form

$$S(\vec{q}_\perp) \sim 1/(q_\perp^2 + \Gamma^2), \qquad (1)$$

where $\vec{q}_\perp$ is measured in the $2k_F$ plane away from the satellite position. The interchain correlation range, defined as $1/\Gamma$, is ~50 Å or five interchain spacings at 80 K. This satellite peak intensity is ~0.05% of the (002) Bragg peak.

The scattering in the vicinity of the (0.5, 0.5, 3.703) satellite position, measured in scans along the [110] direction (scan C of Fig. 1), is shown in Fig. 4 at various temperatures. These data were taken with configuration A of Table I. At 6.5 K, $1/\Gamma = 80$ Å, which is somewhat larger than that found by Renker *et al.* As the temperature is increased to 80 K there is little change in the width and intensity of the scattering, but between 80 and 120 K there is a rapid change, as exemplified by the width and peak intensity in Fig. 2. Note that the peak shape is clearly asymmetric at 120 K. In fact, above 120 K the peak is no longer centered at the zone boundary ($\zeta = 0.5$). We will show that this

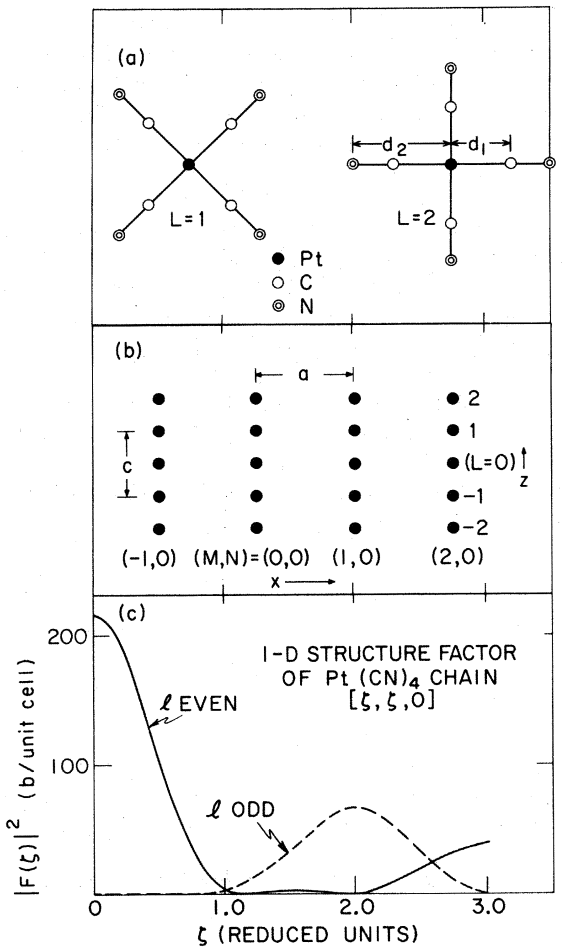

FIG. 5. (a) Planar $Pt(CN)_4$ complexes. Consecutive complexes along the conducting chain axis are rotated by 45°. (b) Schematic diagram of the arrangements of the Pt atoms along and perpendicular to the c axis, with the definition of the coordinate variables shown. The y axis is out of the plane. (c) Square of the one-dimensional structure factor perpendicular to the chain axis for a chain of $Pt(CN)_4$ complexes. The dependence on l is due to the consecutive 45° rotations of the $Pt(CN)_4$.

is due to the dependence of the scattering intensity on the $Pt(CN)_4$ structure factor. At higher temperatures the scattering continues to evolve towards the limiting form expected for a system of uncorrelated chains. The width of the scattering along the c axis, on the other hand, remains narrower than our resolution at all temperatures. The solid curves in the figure are the result of a least-squares fit of the data to the model discussed below.

The observed intensity distribution associated with a given satellite position depends on the atomic displacements caused by the CDW in each chain as well as the correlations between chains. If only the Pt atoms displace, then the structure factor perpendicular to the chain would be a constant, independent of $\vec{Q}_\perp$. If other atoms in the structure also respond to the CDW in each chain, then the structure factor is dependent upon $\vec{Q}_\perp$. A simple and physically very reasonable model is one in which the $Pt(CN)_4$ complexes respond rigidly together to the CDW. Thus, the chains acquire a spatial extent perpendicular to the chain axis, resulting in a variation of the structure factor perpendicular to the c axis. In order to extract an accurate interchain correlation function at various temperatures this structure factor must be taken into account. There is a further complication because the two $Pt(CN)_4$ complexes in the unit cell are not equivalent; alternating $Pt(CN)_4$ planar complexes are rotated by 45° as shown in Fig. 5(a). The structure factors of the two $Pt(CN)_4$ complexes at $z=0$ and $z=\frac{1}{2}$ in the tetragonal unit cell are

$$f_1(\vec{Q}_\perp) = b_{Pt} + 2b_N(\cos Q_x d_2 + \cos Q_y d_2) + 2b_C(\cos Q_x d_1 + \cos Q_y d_1)\,, \tag{2a}$$

and

$$f_2(\vec{Q}_\perp) = b_{Pt} + 2b_N\left[\cos\left(\frac{d_2}{\sqrt{2}}(Q_x+Q_y)\right) + \cos\left(\frac{d_2}{\sqrt{2}}(Q_x-Q_y)\right)\right] + 2b_C\left[\cos\left(\frac{d_1}{\sqrt{2}}(Q_x+Q_y)\right) + \cos\left(\frac{d_1}{\sqrt{2}}(Q_x-Q_y)\right)\right]. \tag{2b}$$

The distances d_1 and d_2 are shown on Fig. 5(a). The scattering lengths of Pt, C, and N are denoted by b_{Pt}, b_C, b_N.

The position of the Lth $Pt(CN)_4$ complex in the chain labeled by (M, N) [see Fig. 5(b)] is given by

$$z_L = \tfrac{1}{2}Lc + A\sin(2k_F\tfrac{1}{2}Lc + \varphi_{M,N})\,, \tag{3}$$

where A is the amplitude, $2k_F$ is the wave vector, and $\varphi_{M,N}$ is the phase of the sinusoidal displacement wave in the chain at (M, N). The elastic-scattering cross section is given by

$$\frac{d\sigma}{d\Omega} = \langle \rho(\vec{Q})\rho^*(\vec{Q})\rangle\,, \tag{4}$$

where

$$\rho(\vec{Q}) = \sum_{\substack{M,N \\ L\ \text{even}}} f_1(\vec{Q}_\perp)\exp\{iQ_z[L\tfrac{1}{2}c + A\sin(2k_F\tfrac{1}{2}Lc + \varphi_{M,N})] + iQ_x Ma + iQ_y Na\}$$
$$+ \sum_{\substack{M,N \\ L\ \text{odd}}} f_2(\vec{Q}_\perp)\exp\{iQ_z[L\tfrac{1}{2}c + A\sin(2k_F\tfrac{1}{2}Lc + \varphi_{M,N})] + iQ_x Ma + iQ_y Na\}\,. \tag{5}$$

The reason for splitting this sum up into odd and even parts is that there are two different $Pt(CN)_4$ complexes per unit cell. As mentioned above there is a tendency for the CDW's in adjacent chains to be 180° out of phase with respect to each other; therefore we set

$$\varphi_{M,N} = (M+N)\pi + \gamma_{M,N}\,. \tag{6}$$

If the interchain correlations were perfect, $\gamma_{M,N}$ would be identically zero, and Bragg reflections would be obtained at the satellite positions

$$\vec{Q}_{CDW} = [l(2\pi/c) \pm 2k_F]\hat{z} + \tfrac{1}{2}(2m+1)(2\pi/a)\hat{x} + \tfrac{1}{2}(2n+1)(2\pi/a)\hat{y}\,. \tag{7}$$

Here $\hat{x}$, $\hat{y}$, $\hat{z}$ are along the $\vec{a}^*$, $\vec{b}^*$, and $\vec{c}^*$ axes, respectively. Since the correlations are not perfect, the relative phases

$$\delta_{M-M',N-N'} \equiv \gamma_{M,N} - \gamma_{M',N'} \tag{8}$$

will have a probability distribution of values about the mean; we must therefore evaluate the ensemble average required by Eq. (4). That is, we must evaluate the phase-phase correlation function

$$\langle\exp[i(\gamma_{M,N} - \gamma_{M',N'})]\rangle = \int P_\delta(M-M', N-N')\, e^{i\delta}\, d\delta\,. \tag{9}$$

The probability that the phase of the CDW in the chain at M, N is in the interval δ to $\delta + d\delta$, given that the phase of the CDW at (M', N') is zero, is $P_\delta(M-M', N-N')\, d\delta$.

In order to calculate the integral in Eq. (9) we need an explicit form for P_δ. We expect P_δ to be-

come progressively broader with increasing interchain separation. To demonstrate the form of the scattering function we take

$$P_\delta(\Delta M, \Delta N) = (1/\sqrt{2\pi}\sigma_{\Delta M,\Delta N}) \times \exp\{-\delta^2/2\sigma^2_{\Delta M,\Delta N}\}, \quad (10)$$

with

$$\sigma^2_{\Delta M,\Delta N} = a^2\sigma_0^2[(\Delta M)^2 + (\Delta N)^2]. \quad (11)$$

Using this P_δ, assuming the amplitude A is small, and performing the sums in Eq. (5), we obtain for the cross section per unit cell in the vicinity of the satellite positions,

$$\frac{d\sigma}{d\Omega} = \frac{Q_g^2 A^2}{8(\sigma_0 a)^2} \sum_l F_l(\vec{Q}_\perp) F_l^*(\vec{Q}_\perp) \sum_{m,n} \exp\left(-\frac{[Q_x - (m+\frac{1}{2})2\pi/a]^2}{2\sigma_0^2}\right) \exp\left(-\frac{[Q_y - (n+\frac{1}{2})2\pi/a]^2}{2\sigma_0^2}\right) \delta(2\pi l \pm 2k_F c - Q_z c). \quad (12)$$

where

$$F_l(\vec{Q}_\perp) = [f_1(\vec{Q}_\perp) + (-1)^l f_2(\vec{Q}_\perp)]. \quad (13)$$

A plot of the square of this structure factor is shown in Fig. 5(c) for $\vec{Q}_\perp$ along [110]. Since each term in the sum over m and n is a Gaussian-shaped satellite peak which is symmetric, the observed asymmetry of the peaks shown in Fig. 4 comes solely from the variation of $F_l(\vec{Q}_\perp)$ across the peak. In order to compare this cross section with experiment it must be convoluted with the instrumental resolution. Since the Q_z width of the cross section is much smaller than the resolution, this convolution reduces to a two-dimensional integral in the $2k_F$ planes. To determine the parameters A and σ_0, a least-squares fit to the data was made. We have found that a Lorentzian [Eq. (1)], with $\sigma_0 \to \Gamma$, is better than the Gaussian form of Eq. (12), as previously mentioned.

The overall fit of the data shown in Fig. 4 is very good. In particular, the observed asymmetry of the peaks is predicted accurately. It is clear from Eqs. (12) and (13) that this asymmetry comes solely from the rapid variation of $F(\vec{Q}_\perp)$ along the [110] line [Fig. 5(c)], and not from the interchain correlation function.

The results of the fitting for the amplitude A of the sinusoidal atomic displacement wave and the inverse correlation length Γ are shown in Fig. 6. The amplitude A has been put on an absolute scale by using the value determined by Ref. 14 at 7 K. The amplitude remains constant with increasing temperature up to 80 K, and then gradually begins to fall off at higher temperatures. Based on the thermal factors obtained by Peters and Eagen[15] in their crystal-structure refinements, part of this decrease is attributable to a Debye-Waller factor. The amplitude A would be 15% larger than shown in Fig. 6 at 300 K if this effect was taken into account. The error bars shown for $A(T)$ and $\Gamma(T)$ were determined by the reproducibility of the results for data taken with different resolution conditions and at different satellite positions. Figure 7 shows the fits for several different values of $\vec{Q}_{CDW}$ under the same instrumental conditions as for Fig. 4. The results for A and Γ fall within the error bars shown in Fig. 6.

We should point out that using a Lorentzian in place of a Gaussian in Eq. (12) presents certain mathematical difficulties. A Lorentzian in two dimensions is not normalizable, and thus the scattering cross section integrated over Q_x and Q_y would appear to diverge. By Fourier inversion the resulting form for P_δ is also not normalizable. This problem can be circumvented by various schemes; for example, by cutting off the Lorentzian at some large $\vec{Q}$. However, in our numerical fitting procedure, these conceptual difficulties are not important. The widths of the peaks determine Γ and the heights are proportional to A^2/Γ^2.

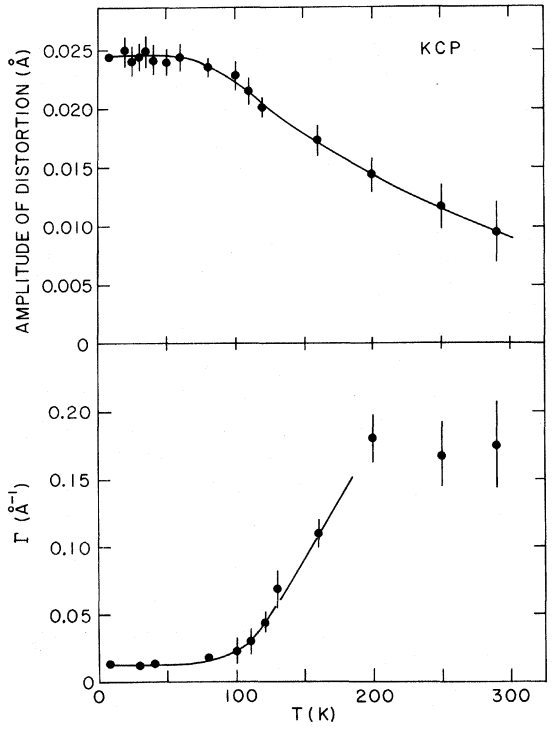

FIG. 6. Temperature dependence of the amplitude of the sinusoidal CDW in each chain and the inverse correlation range perpendicular to $\vec{c}$ for the model discussed in the text. The solid lines are simply a guide to the eye.

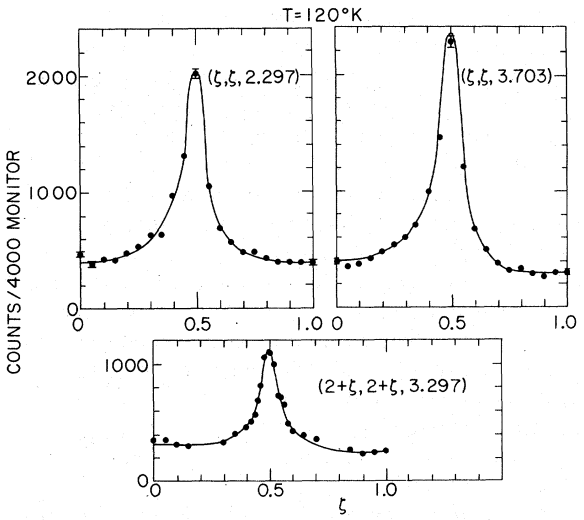

FIG. 7. Elastic scattering at 120 K for several different CDW satellite positions. The solid curves are the fits to the model described in the text. The observed asymmetry is due to the variation of the $Pt(CN)_4$ structure factor perpendicular to $\vec{c}$.

IV. INELASTIC-SCATTERING RESULTS

We now turn our attention to the dynamics. The 1 – D properties are expected to show up in the inelastic scattering as well as the elastic scattering. Above the temperature at which a static sinusoidal CDW state occurs a Kohn anomaly may be found in the phonon spectrum for wave vectors in the vicinity of the $2k_F$ plane.[16] As the temperature decreases the phonons would then soften and finally trigger the sinusoidal distortion. According to this soft-mode concept the energy of this branch would then increase in energy below the transition. As discussed in the introduction, Renker *et al.*[5] observed an anomaly in the longitudinal phonon spectrum along the *c* axis direction which they interpreted as a giant Kohn anomaly. The subsequent observation[7] of an elastic component to the scattering at room temperature indicated that either a Peierls-type transition had already taken place, or that the elastic scattering was analogous to the "central modes" observed in other materials and was therefore a prelude to the distortion.[17] The rapid variation of the satellite peak intensity and width around 100 K as shown in Fig. 2 has been identified as a Peierls transition.[1,2,18,19]

To clarify the nature of the inelastic scattering in the vicinity of the $2k_F$ instability, we have investigated the temperature dependence of this scattering. At room temperature we find that the scattering in the vicinity of the anomaly extends lower than previously observed, and appears to be connected in a continuous fashion to the elastic scattering all along the $2k_F$ plane. Furthermore, as

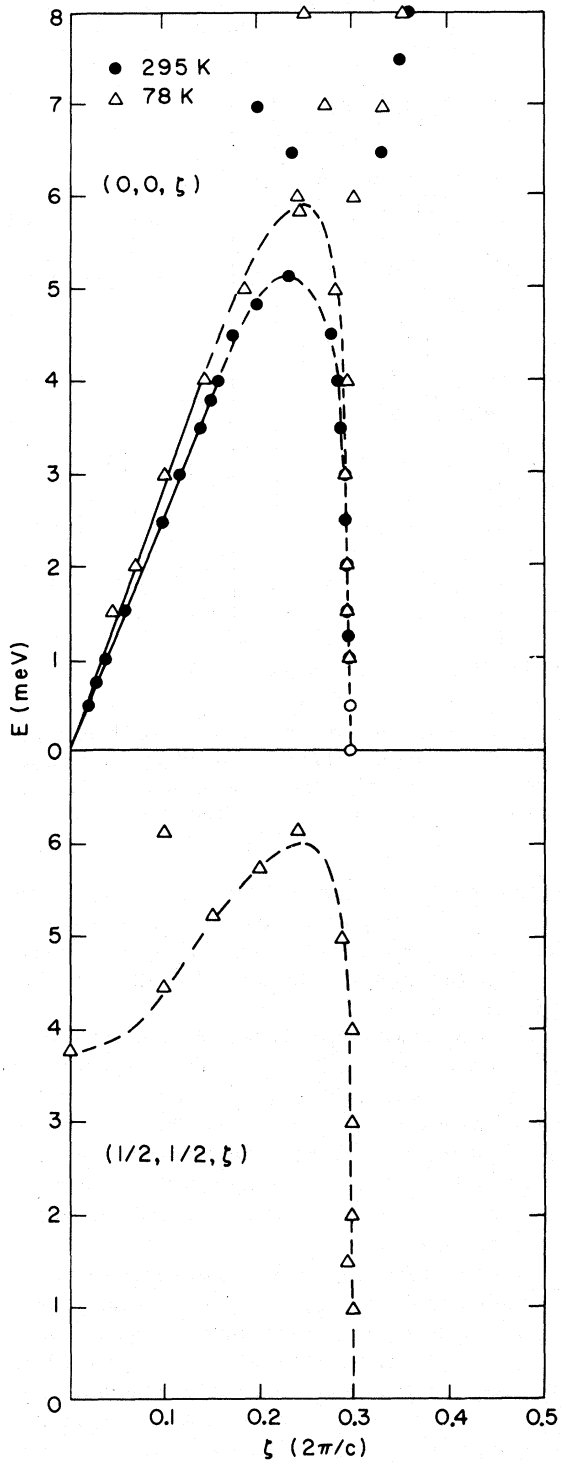

FIG. 8. Inelastic cross section for phonons with primarily *c*-axis polarization: (a) along the *c*-axis at room temperature and 78 K; (b) along the zone boundary in the *c*-axis direction at 78 K. The steep descent around $\zeta = 0.3$ is the $2k_F$ anomaly. The inelastic scattering appears to extend continuously down to $E \approx 0$. The dashed curves are intended as a guide to the eye, and near $2k_F$ should not necessarily be regarded as the "phonon dispersion relation."

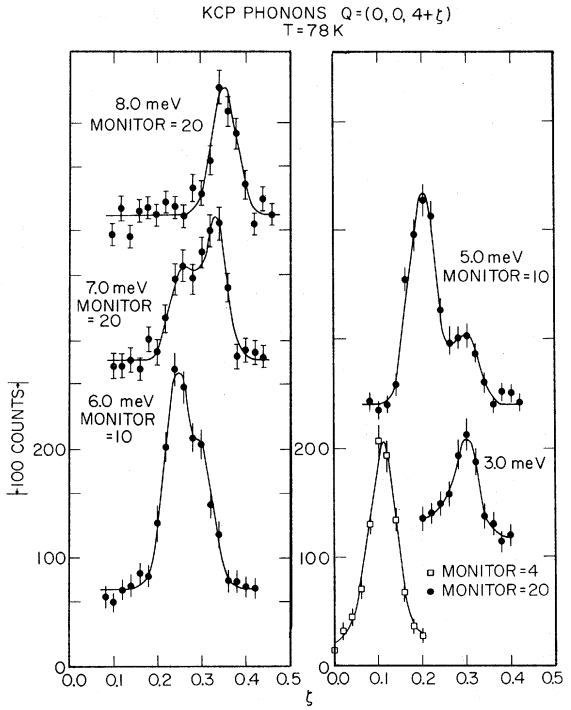

FIG. 9. Series of constant-energy-transfer measurements at 78 K in the vicinity of a $2k_F$ plane. The effective counting time is proportional to the monitor. The solid lines are least-squares fits of the data to Gaussian's.

the temperature is lowered through T_{3D} no qualitative change in the phonon spectrum is observed. The increase in the interchain correlations therefore does not appear to be directly related to the CDW distortion in the chains.

Figure 8 shows the inelastic cross section for phonons with polarizations primarily along the c-axis direction. Figure 8(a) gives the dispersion relation on the c axis, as in scan B of Fig. 1, at room temperature and at 78 K. The steep descent near $\zeta = 0.3$ is due to the $2k_F$ anomaly. The transverse acoustic phonon along the [001] direction shows no such large anomaly.

Since the scattering near $2k_F$ is very steep, the constant-Q method of scanning (i.e., fixing the momentum transfer and varying the energy transfer) was not a satisfactory method. We have therefore taken the majority of our measurements around $2k_F$ by fixing the energy transfer and varying the momentum transfer (constant-E scans). A series of these types of scans is shown in Fig. 9 from 3 to 8 meV for $T = 78$ K. Note that with increasing energy the ratio of the intensity of the longitudinal acoustic (LA) phonon to the $2k_F$ scattering increases. At energies higher than 6 meV though this separation into the LA phonon and $2k_F$ scattering does not appear to be viable. Our sample size was not sufficiently large to unambiguously determine the nature of the scattering above 6 meV, but it appears there may also be scattering from an optical mode in this region. We hope to clarify this point when a larger single crystal becomes available.

The cross section on the zone-boundary line [0.5 0.5 ζ] is shown in Fig. 8(b) for $T = 78$ K. At $\zeta = 0$ the phonon is the transverse zone-boundary phonon in the [110] direction. Proceeding in the [001] direction from this point (ζ increasing) we find the same type of scattering as along the c axis. Note that (0.5, 0.5, 0.297) is where CDW scattering has built up. The same type of scattering is observed above T_{3D}. The dispersion curve has also been measured for (0.25, 0.25, ζ), with similar results. Clearly the inelastic scattering near $Q_z = 2k_F$ is 1 – D in nature, in agreement with previous results.[5,18]

Figure 10 shows the observed inelastic scattering for several representative scans at 215 K. Figure 10(a) is the LA [001] phonon at an energy transfer of 2.0 meV. Figure 10(b) is an identical scan along the c axis through the $2k_F$ plane (scan B of Fig. 1). The ratio of the peak intensities is 28 : 1. Figure 10(c) shows that the scattering along the [110] zone boundary is considerably stronger in in-

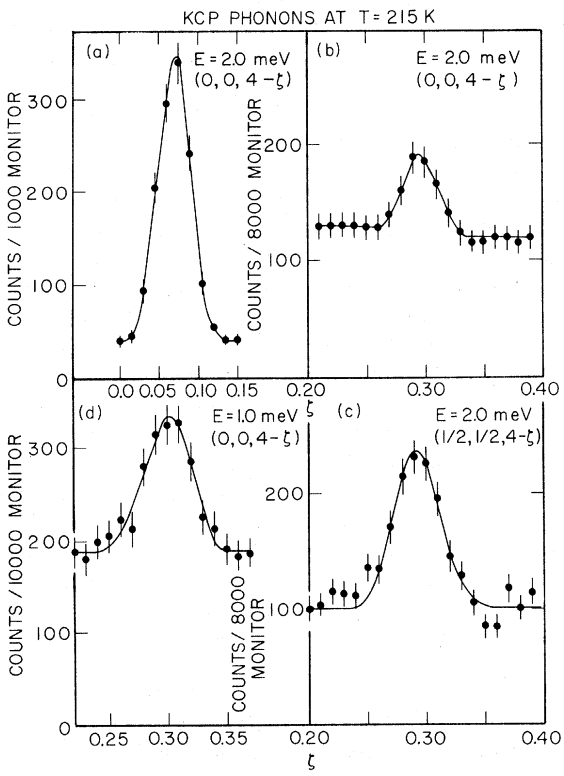

FIG. 10. Several constant-energy-transfer scans at 215 K: (a) [001] LA phonon; (b) $2k_F$ scattering along the c axis; (c) $2k_F$ scattering at the intersection of the $2k_F$ plane and the [110] zone boundary, where the CDW elastic scattering develops at low temperatures; (d) same as (b).

tensity than directly along the c axis, whereas the inelastic scattering at (1, 1, $2k_F$) was unobservable. In general, we have found that the inelastic and elastic $2k_F$ intensities are qualitatively proportional to each other. That is, the inelastic $2k_F$ scattering is most easily observable in the regions of $\vec{k}$-space where the elastic CDW scattering is largest. Figure 10(d) displays the inelastic scattering along the c axis for an energy transfer of 1.0 meV. The half-width energy resolution for this scan is 0.35 meV, so the contribution to the scattering from $E = 0$ is very small, as evidenced from the low background. At energy transfers less than 1.0 meV the contribution from the elastic scattering under these conditions is not small, and this results in a rapid increase in the background (from elastic incoherent scattering) as well as contributions from the elastic $2k_F$ scattering. The room-temperature measurements near the $2k_F$ anomaly for 0.5 and 0.0 meV energy transfers are shown in Fig. 8(a) as open circles to denote this resolution effect.

Figure 11 shows the inelastic scattering for a series of temperatures above and below T_{3D} at an energy transfer of 2.0 meV. The scattering continuously increases in intensity with increasing temperature. This is shown in Fig. 12, where we have plotted the observed intensity at 2.0 meV as

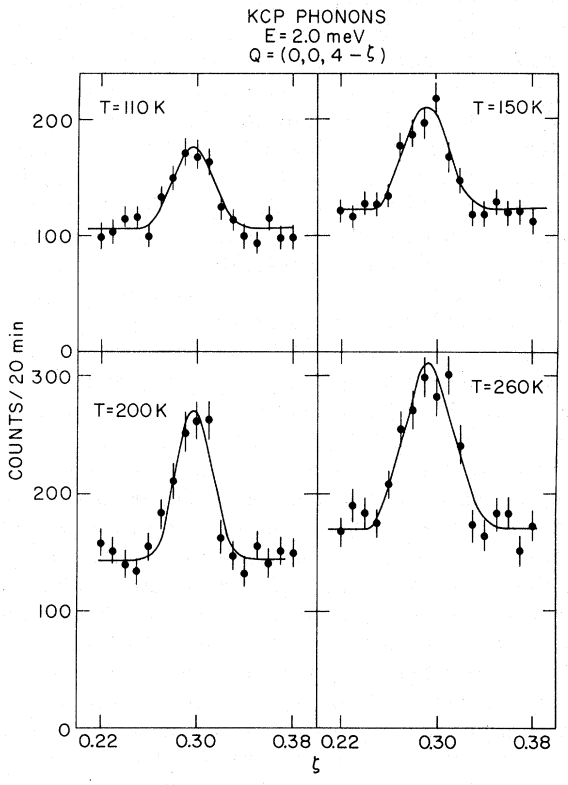

FIG. 11. Observed inelastic scattering at temperatures above and below T_{3D} for an energy transfer of 2 meV in the vicinity of the $2k_F$ plane.

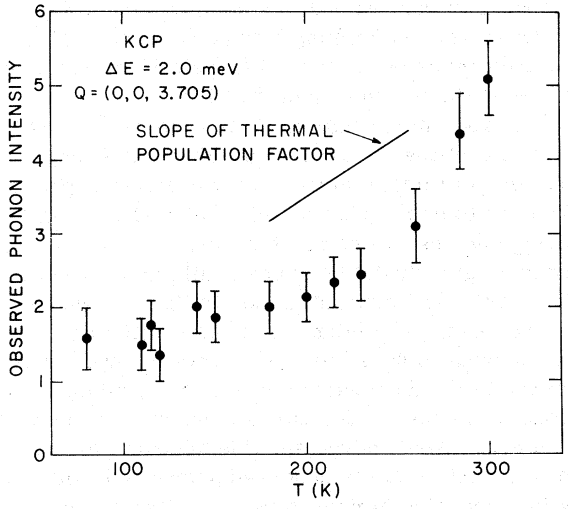

FIG. 12. Temperature dependence of the intensity of the inelastic scattering at an energy transfer of 2 meV. The intensity increases monotonically with temperature and shows no evidence of the interchain correlations rapidly developing below 120 K.

a function of temperature. There is no qualitative change in the scattering over the temperature range covered.

To compare the intensities measured in these $2k_F$ scans as a function of energy and temperature, one must keep in mind that phonon intensities in constant-E scans are not as readily compared with each other as in constant-Q scans. If the scattering is due to well-defined phonons, then the intensity $I(E)$ is given by[20,21]

$$I(E) \sim \frac{n(E/kT)\rho(E)}{E} |F|^2 e^{-2W(\vec{Q})}, \tag{14}$$

where $n(E/kT)$ is the Bose thermal-population factor, $\rho(E)$ is the density of phonon states contributing to the intensity (which is inversely proportional to the slope of the dispersion curve), $|F|^2$ is the phonon structure factor, and $e^{-2W(\vec{Q})}$ is the Debye-Waller factor. The scattering near $2k_F$ is then complicated by the fact that there are two branches contributing to these constant-E scans. These two peaks are not experimentally resolvable; so the slope of the dispersion curve is not yet known, and the temperature and wave-vector dependence of the phonon-structure factor is unknown. Moreover, we have little information on the effects of damping of the phonons as well as the mixed electronic-vibrational character of the modes near $2k_F$. In this case, Eq. (14) is not directly applicable, and using the term phonon to describe the scattering can be misleading. The scattering around $2k_F$ is too steep for us to cleanly separate the effects of damping and dispersion. Finally, the neutron-scattering cross section in the vicinity of $2k_F$ does not

necessarily correspond to a normal mode excitation of the system with a single wave vector $\vec{q}$. This is a consequence of the loss of translational periodicity due to the incommensurate CDW.

A unique interpretation of the observed intensity variation of the inelastic scattering with energy and temperature is clearly very difficult at present. We hope to better characterize the inelastic scattering and resolve some of these problems when a large single crystal becomes available. However, there are some general trends to the data which can be seen. The intensity of the scattering near $2k_F$ decreases with decreasing energy, while concurrently the dispersion becomes very steep. The slope of the dispersion curve thereby increases with decreasing energy and this accounts for at least a portion of the observed decrease of intensity. With increasing temperature, the intensity at low energies increases monotonically (Fig. 12), but not as rapidly as expected from the variation of the thermal population factor alone. For comparison we measured the intensity of the LA phonon at each temperature, and found that this intensity increased only slightly less than that expected from $n(E/kT)$. We attributed this to the temperature dependence of the Debye-Waller factor.

V. DISCUSSION

The MVPC as well as the charge-transfer salts of TCNQ which have 1 – D conducting properties at room temperature have all been found to be good dc electrical insulators at low temperatures.[1] A number of models have been proposed[1] to explain the contrasting behaviors of the dc and optical conductivities. The models assume different mechanisms for the electron localization at low temperatures, but they often take advantage of the enhanced sensitivity of 1 – D systems to the effects of fluctuations, impurities, defects, and disorder.[19,22–24] The electron localization is, however, not necessarily restricted to an atomic scale, and, in fact, experiments indicate that this is not the case.[25] The interrupted strand model,[22] for example, assumes that there are metallic strands which are interrupted by lattice defects, the defects introducing energy barriers in the strands which restrict electron movement at low temperatures. Such a defect model could also explain why complete 3 – D ordering is not achieved. If there is a CDW in each strand, then any defects present would tend to "pin" the CDW and introduce a random phase shift between strands which would inhibit the 3 – D order. Although the cause of the incomplete ordering has not yet been experimentally extablished, it appears to us that there are two possible explanations for the broadening of the CDW peaks with increasing temperature. One is that the pinning energy of the CDW in the chains is temperature dependent. This would allow the relative dephasing of static atomic displacement waves in the chains. The most likely explanation, though, is that the dephasing is due to very low-frequency fluctuations, that is, to phason modes as discussed by Overhauser.[26] It is possible that the apparent absence of complete order at very low temperatures is really the result of the zero-point motion of these low-lying excitations. The neutron-spectrometer energy resolution is large compared to these excitations, and therefore integrates over them. Thus, the CDW scattering would appear to be elastic and broadened.

According to the simple models of the Peierls distortion[3] the amplitude A of the CDW is directly proportional to the electron-energy gap. Our results for A show that it decreases gradually with increasing temperature above ~80 K. The energy gap inferred on the basis of a thermal-activation model for the dc conductivity is in qualitative agreement with this variation, but the gap falls off much more rapidly with temperature. The gap as determined from optical measurements,[1,2] on the other hand, shows no temperature dependence. However, these results are not inconsistent with each other since for physically more realistic models these quantities measured by different techniques are not expected to be proportional to each other.

Many of the basic characterizations of the scattering which we observe, such as the variation with temperature of the intensity and width of the CDW satellite scattering, are in agreement with the results of Renker *et al.*[5,7] At room temperature we also obtain similar results for the ratios of the intensities of the LA phonon to the $2k_F$ scattering where the data overlap. However, we are able to measure the inelastic scattering to lower-energy transfers and thereby determine the relationship between the elastic and inelastic cross sections. These results led us to a somewhat different interpretation of the nature of the scattering.

Recently, Renker *et al.*[18] have reported a dramatic change in the phonon spectrum just above T_{3D}. At 150 K they report that the spectra at $2k_F$ starts to develop a typical phonon line and at 130 K only a flat dispersion curve remains where the large $2k_F$ anomaly was found at room temperature. They have interpreted this as evidence of a phonon condensation which produces a truly static Peierls distortion below T_{3D}; the electron-energy gap then suppresses the $2k_F$ anomaly as well as phonon damping. Our results are in disagreement with this. We find that there is no qualitative change in the phonon spectrum near T_{3D}. We believe that there is no phase transformation taking place, but that there is only an increase in the interchain correlations. The source of this disagreement is not known. Clearly more inelastic scattering work is necessary.

The effects of fluctuations are known to be important for 1 – D systems. An ideally 1 – D system in the absence of infinite range forces does not have a phase transition at finite temperatures,[27] but weak 3 – D interactions can induce a transition. Lee, Rice, and Anderson[19] have calculated the effects of fluctuations of the order parameter on the Peierls transition and found that a 3 – D transition should occur at $T_{3D} \sim \frac{1}{4} T_C$, where T_C is the mean-field transition temperature. Identifying this T_{3D} with the T_{3D} for KCP and using a tight-binding band width of ~1 eV, they estimated an intrachain correlation length ξ at room temperature of ~7 Pt atoms, which is considerably less than the lower limit of 60 Pt atoms set by Comes *et al.*[6] or the limit of over 100 Pt atoms we have set for $T \lesssim 160$ K. More recently, Levin *et al.*[24] have suggested that T_{3D} should be $\sim \frac{1}{20} T_C$, which would yield values of ξ more in line with experiment, but would give $T_C \sim 2000$ K, which is considerably larger than expected on the basis of optical measurements.[2] Sham and Patton[23] have estimated ξ (300 K) ~ 25 Pt atoms, and ξ (6 K) ~ 200. We would like to point out that our results in no way rule out the possibility that 3 – D interactions induce the linear distortion.

Recently, CDW's have been discovered in several other materials, such as $TaSe_2$,[28] VS,[29] NbO_2.[30] In this paper we have emphasized the 1 – D properties of KCP, but it is likely that a broader perspective of CDW's and their associated fluctuations should be taken.

ACKNOWLEDGMENTS

The authors have benefited greatly from numerous discussions with our colleagues at various laboratories: A. W. Overhauser (Purdue); T. M. Rice (Simon Fraser); J. D. Axe, M. Blume, V. Emery, and R. Pynn (Brookhaven); C. F. Eagen, R. C. Jaklevic, and C. Peters (Ford); F. DiSalvo, J. Wilson, and C. Varma (Bell); S. W. Peterson, J. Williams (Argonne); A. Luther (Harvard). They are particularly grateful to L. C. Davis (Ford) for mathematical assistance on phase-phase correlations.

---

*On leave from Japan Atomic Energy Research Institute.

†Neutron scattering work performed at Brookhaven National Laboratory under the auspices of the U. S. Energy Research and Development Administration.

‡Single-crystal samples prepared at Scientific Research Staff, Ford Motor Co.

[1]In order to avoid an extensive list of references, we refer to the reviews by H. R. Zeller, Vol. XIII of *Festkorperprobleme*, p. 31 (1973); I. F. Schegolev, Phys. Status Solidi (a) 12, 9 (1972); K. Krogmann, Ang. Chem. Int. Ed. Engl. 8, 35 (1969).

[2]H. R. Zeller and P. Bruesch, Phys. Status Solidi (b) 65, 537 (1974); P. Bruesch, S. Strassler, and H. R. Zeller, 12, 219 (1975).

[3]R. E. Peierls, *Quantum Theory of Solids*, (Clarendon, Oxford, 1964), p. 108.

[4]R. Comes, M. Lambert, H. Launois, and H. R. Zeller, Phys. Rev. B 8, 571 (1973).

[5]B. Renker, H. Rietschel, L. Pintschovius, W. Glaser, P. Bruesch, D. Kuse, and M. J. Rice, Phys. Rev. Lett. 30, 1144 (1973).

[6]R. Comes, M. Lambert, and H. R. Zeller, Phys. Status Solidi (b) 58, 587 (1973). R. Comes, in *One-Dimensional Conductors*, edited by H. G. Schuster (Springer-Verlag, 1975), p. 32.

[7]B. Renker, L. Pintschovius, W. Glaser, H. Rietschel, R. Comes, L. Liebert, and W. Drexel, Phys. Rev. Lett. 32, 836 (1974).

[8]The recent crystal-structure work shows that KCP is noncentrosymmetric; see J. M. Williams, J. L. Peterson, H. M. Gerdes, and S. W. Peterson, Phys. Rev. Lett. 33, 1079 (1974); H. J. Deiseroth and H. Schulz, Phys. Rev. Lett. 33, 963 (1974). The work of C. R. Peters and C. F. Eagen (Ref. 15) reveals that the full complement of waters of hydration is 3.2 H_2O. The extra 0.2 H_2O per formula unit occupy the unit cells where Br is absent. It should be pointed out that Deiseroth and Schulz's terminology in calling the odd-l main Bragg reflections superstructure reflections is very misleading in a material where there are CDW satellites.

[9]M. J. Cooper and R. Nathans, Acta Cryst. 23, 357 (1967).

[10]R. B. Saillant, R. C. Jaklevic, and C. D. Bedford, Mater. Res. Bull. 9, 389 (1974).

[11]D. Griffiths, P. Day, C. F. Sampson, and F. A. Wedgewood, Solid State Commun. (to be published).

[12]M. Barmatz, L. R. Testardi, A. F. Garito, and A. J. Heeger, Solid State Commun. 15, 1299 (1974).

[13]A. Menth and M. J. Rice, Solid State Commun. 11, 1025 (1972).

[14]C. F. Eagen, S. A. Werner, and R. B. Saillant (unpublished).

[15]C. Peters and C. F. Eagen (Phys. Rev. Lett. 34, 1132 (1975).

[16]See, for example, M. J. Rice and S. Strassler, Solid State Commun. 13, 125 (1973); H. Rietschel, *ibid.* 14, 699 (1974); J. J. Hopfield, 14, 727 (1974); B. Horovitz, M. Weger, and H. Gutfreund, Phys. Rev. B 9, 1246 (1974).

[17]G. Shirane, Rev. Mod. Phys. 46, 437 (1974).

[18]B. Renker, L. Pintschovius, W. Glaser, H. Rietschel, and R. Comes, in *One-Dimensional Conductors*, edited by H. G. Schuster (Springer-Verlag, 1975), p. 53.

[19]P. A. Lee, T. M. Rice, and P. W. Anderson, Phys. Rev. Lett. 31, 462 (1973); Solid State Commun. 14, 703 (1974).

[20]B. N. Brockhouse, L. N. Becka, K. P. Rao, and A. D. B. Woods, in *Second Symposium on Inelastic Scattering of Neutrons in Solids and Liquids* (IAEC, Vienna, 1963), Vol. II, p. 23.

[21]W. Marshall and S. W. Lovesey, *Theory of Thermal Neutron Scattering* (Oxford, London, 1971).

[22]D. Kuse and H. R. Zeller, Phys. Rev. Lett. 27, 1060 (1971); M. J. Rice and J. Bernasconi, J. Phys. F 3, 55 (1973).

[23]See, for example, D. J. Scalapino, M. Sears, and R. A. Ferrell, Phys. Rev. B 6, 3409 (1972); A. N.

Bloch, R. B. Weisman, and C. M. Varma, Phys. Rev. Lett. 28, 753 (1972); A. Luther and I. Peschel, *ibid.* 32, 992 (1974); B. R. Patton and L. J. Sham, *ibid.* 33, 638 (1974); S. T. Chui, T. M. Rice, and C. M. Varma, Solid State Commun. 15, 155 (1974); A. Madhukar, *ibid.* 15, 921 (1974); P. N. Sen and C. M. Varma, *ibid.* 15, 1905 (1974); M. C. Leung, *ibid.* 15, 879 (1974); A. Luther and V. J. Emery, Phys. Rev. Lett. 33, 1589 (1974); L. J. Sham and B. R. Patton (unpublished).

[24]K. Levin, S. L. Cunningham, and D. L. Mills, Phys. Rev. B 10, 3832 (1974).

[25]W. Ruegg, D. Kuse, and H. R. Zeller, Phys. Rev. B 8, 952 (1973).

[26]A. W. Overhauser, Phys. Rev. B 3, 3173 (1971).

[27]P. C. Hohenberg, Phys. Rev. 158, 383 (1967).

[28]J. A. Wilson, F. J. DiSalvo, and S. Mahojan, Adv. Phys. 24, 117 (1975); D. E. Moncton, J. D. Axe, and F. J. DiSalvo, Phys. Rev. Lett. 34, 734 (1975).

[29]S. H. Liu, Phys. Rev. B 10, 3619 (1974).

[30]R. Pynn, J. D. Axe, and R. Thomas (unpublished).